

# P1B.10 Ka-band radar observations of orographic snow clouds and flows across a steep mountain ridge

Kenichi Kusunoki <sup>1\*</sup>, Masataka Murakami <sup>1</sup>, Narihiro Orikasa <sup>1</sup>, Yoshinobu Tanaka <sup>1</sup>, Koyuru Iwanami <sup>2</sup>, Masayuki Maki <sup>2</sup>, Park SangGoon <sup>2</sup>, Ryohei Misumi <sup>2</sup>, Kyosuke Hamazu <sup>3</sup>, and Hiroshi Kosuge <sup>4</sup>

<sup>1</sup> Meteorological Research Institute, Japan

<sup>2</sup> National Research Institute for Earth Science and Disaster Prevention, Japan

<sup>3</sup> Radio Atmospheric Science Center, Kyoto University, Japan

<sup>4</sup> Tone River Dams Integrated Control Office, Ministry of Land, Infrastructure, and Transport, Japan

## 1. Introduction

An understanding of flows and precipitation over orography is important for a number of purposes. While extensive model studies have been conducted, there have been relatively few observational studies.

On the western side of the central mountain range of Japan, namely, on the coast of the Sea of Japan, a unique mesoscale climate exists during winter. The cold northwesterly monsoon, accompanied by a strong Siberian high and active cold surges, persists and blows over the Sea of Japan, which has relatively warmer temperature. Shallow convective clouds appear in a well-mixed layer over the Sea of Japan, advect southeastward, and land at the Japan Sea side. The several hundred-km length of the mountain chain forms a natural barrier to the moisture-laden airmass of the winter monsoon, and heavy snowfall frequently occurs. Such an incoming airmass influenced by local orographic effects can provide an excellent setting for studying the evolution of orographic snow clouds. This paper documents the influence of orographic features on snow clouds around the Mikuni Mountains, Japan, for a case of relatively steady northwesterly monsoon flow. In this study, the data from the Ka-band Doppler radars provided unique datasets, which were used to analyze detailed flow and precipitation structures.

## 2. The study area and instrumentation

### a. The local terrain of the study area

Figure 1 shows the locations of the instruments and the surrounding terrain. The area consists of mountains, a basin, and a valley, and the elevation varies from about 150m to 2000m. The primary data used for this study are radar data collected by two Ka-band Doppler radars at the windward radar site (Senjoji) and the leeward radar site (Hodaigi), respectively. The radars were deployed along the NW-SE line, which corresponded to the common direction of the winter monsoon. The distance from the windward radar site to the leeward radar site was 32km. The ridge of the Mikuni Mountains was at the

---

\* *Corresponding author address:* Kenichi Kusunoki, Meteorological Research Institute, Tsukuba, Japan; e-mail: [kkusunok@mri-jma.go.jp](mailto:kkusunok@mri-jma.go.jp).

midpoint between both radar sites. To examine the upstream conditions, rawinsondes were launched 15 km upstream from the ridge at 0827, 1141, and 1520 JST (Japan Standard Time). The deployment of instruments is suitable for the primary interest, which is to focus on the nature of the orographically modified flows to snow clouds and flows around a steep mountain ridge.

### b. The Ka-band Doppler radars

The Ka-band Doppler radar located at the leeward radar site was developed in 1996 by the Mitsubishi Electric Corporation (MELCO) and the Radio Atmospheric Science Center (RASC) of Kyoto University. The radar located at the windward site is a greatly improved version of the leeward radar (Iwanami et al. 2001). The advantage of millimeter-wavelength radars over centimeter weather radars (with the same size antennas and transmitting powers) are finer spatial resolution and more sensitivity to smaller particles. One limitation of millimeter-wavelength radars is attenuation by rain, but we conclude that the attenuation could be ignored because of the dry snowfall event.

In this work, radar data from RHI scans of 135.0 azimuth of the windward radar and 315.0 azimuth of the leeward radar were used, as the direction along the line of radar sites and the flows of the winter monsoon.

## 3. Synoptic overview and upstream conditions

During the study period, a nearly east-west pressure gradient, that is the typical pattern when the winter monsoon prevails around Japan, appeared between a strong Siberian high and the cyclone over the Pacific Ocean. The wind hodographs derived from the upstream soundings (Fig. 2) indicate that the wind speed increased with height and the mean wind direction was northwesterly, which was along the radar sites. The upstream Froude number (Fr) and non-dimensional mountain height were calculated from these soundings (Fig. 3). The Frs were 0.30 (at 0827 JST), 0.36 (at 1140 JST), and 0.7 (at 1520 JST), respectively, as should be expected to develop critical flows over the ridge and a hydraulic jump over the leeward side.

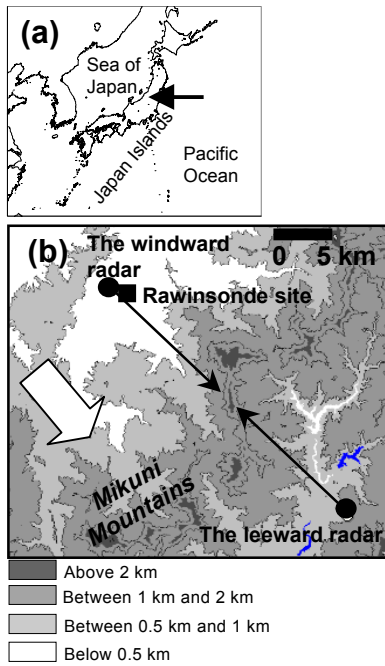


Fig. 1 (a) Map showing the location of the study area (the tip of the black arrow). (b) Enlarged map around the study area including terrain contours every 250m. The locations marked by the symbols are as follows: the windward and the leeward radar sites (circles); rawinsonde site (square). The white arrow shows the direction of the monsoon flow. The RHI scan beams of each radar are indicated by thin arrows.

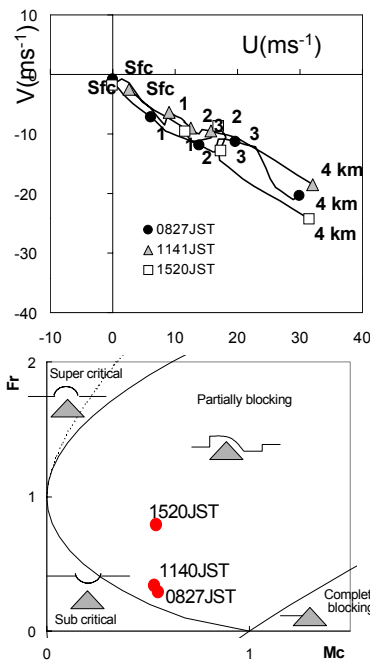


Fig. 2 Wind hodographs at 15km upstream from the mountain ridge.

Fig. 3 Upstream Froude numbers derived from the three soundings.

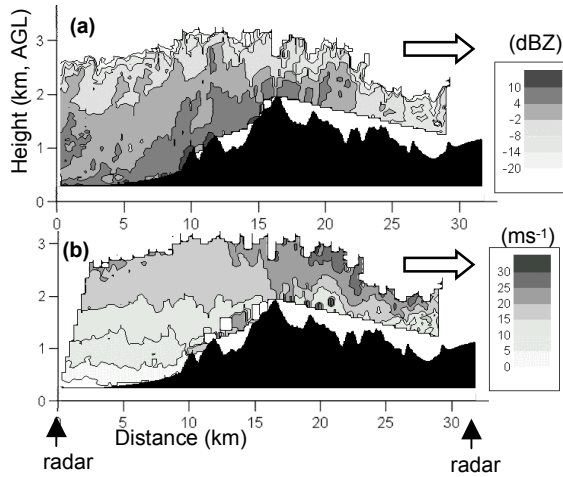


Fig. 4 Composites of (a) reflectivity and (b) Doppler velocity along the NW-SE vertical plane. The arrow shows the direction of the monsoon flow. Note that the signs of Doppler velocity of the leeward side radar are reversed.

#### 4. Results

In order to examine the flows and precipitation around the Mikuni Mountains, the composites of the reflectivity and Doppler velocity between the windward and leeward scans were made. These composites were along the NW-SE vertical plane and constructed from RHI scans (oriented 315-135). Figure 4 shows an example of the composites. The reflectivity composite suggests that the snow clouds were rising over the windward barrier, passing over the ridge, and descend on the leeward side of the Mikuni Mountains. The Doppler velocity composite indicates the relatively laminar flows on the windward side became turbulent when the flows past the mountain ridge. In order to remove fluctuations with snapshots, the composites were averaged during the study period (Fig. 5). Furthermore, to compare the flow regime in the different Fr conditions, the study period was divided into two periods around the period when no data were available (i.e., 14 -15 JST). The first period (hereafter Period I) is from 09JST to 13JST, when the upstream Froude number was relatively small (less than 0.4). The second period (hereafter Period II) is from 15JST to 16JST, when the upstream Froude number was relatively large (greater than 0.4). The echo top heights and the Doppler velocity distributions at 2km height (i.e., the mountain height) were averaged during Period I and Period II, respectively (Fig. 6).

##### a. Upstream influence of the ridge

The averaged composite of reflectivity highlights the precipitation enhancement on the windward slope that would generate orographic rising (Fig. 5 (a)). Fig. 6 (a) shows that the trends of echo top height on the windward side are opposite between the two periods; the echo top height decreased (increased) near the ridge during Period I (Period II). The averaged Doppler velocity distributions at 2km height (Fig. 6 (b)) indicate that the horizontal wind speed on the windward side increased (decreased) near the ridge during Period I (Period II). Figure 7 shows the examples of the time series of radar reflectivity. The echo cells moved almost directly across the ridge during the period II. However, during the period I, the reflectivity peak remained on the windward slope ; in other words, the echo cell tracks were discontinuous around the

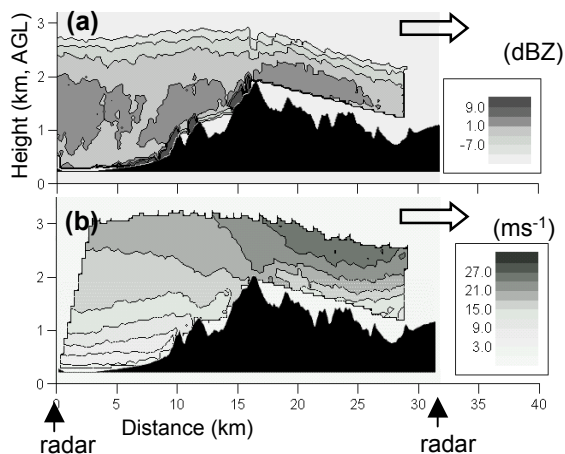


Fig. 5 Same as Fig. 4 but averaged during the study period.

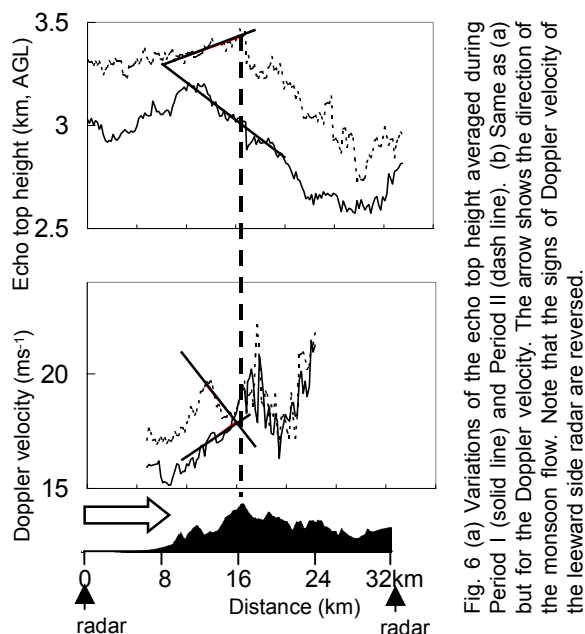


Fig. 6 (a) Variations of the echo top height averaged during Period I (solid line) and Period II (dash line). (b) Same as (a) but for the Doppler velocity. The arrow shows the direction of the monsoon flow. Note that the signs of Doppler velocity of the leeward side radar are reversed.

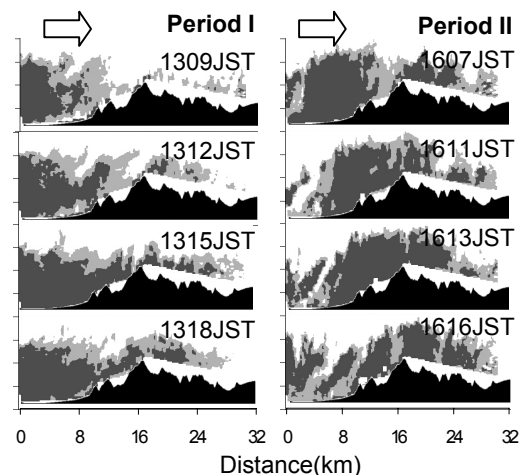


Fig. 7 The time series of composite radar refractivity. The arrow shows the direction of the monsoon flow.

ridge. PPI scan reflectivity image averaged during the period I indicates that the radar reflectivity was stronger around the ridge rather than overt the ridge, suggesting echo cells during the period I was diverted on the windward slope and flowed around the ridge (not shown).

### b. Mountain wake over the leeward slopes

#### 1) MODULATION OF AIRFLOW

The NW-SE line at 2.0 km AGL (i.e., the mountain height) versus time series of the Doppler velocity is indicated in Fig. 8. This time series shows apparently the transition from the laminar flows to turbulent flows at the ridge. Furthermore, this figure indicates an acceleration of the downslope flow to 27.0  $\text{ms}^{-1}$  adjacent to the ridge and a deceleration of the flow to 16.0  $\text{ms}^{-1}$  over the lee slope approximately 5 km from the ridge. The acceleration and the deceleration of the flow over the lee slope are also indicated in Fig. 6 (b), suggesting the flow accelerated to a supercritical speed followed by a hydraulic jump-like transition over the lee slope. Figure 9 shows an example of PPI scan of Doppler velocity from the leeward radar at 0934 JST. It is evident that an elongated region of weak Doppler velocity behind the ridge. This region shows pronounced kinks, suggesting that positive and negative vortices had formed behind the ridge and were shed downstream quasi-periodically. The nondimensional shedding frequencies were calculated as 0.2-0.4, which agrees with previous studies obtained based on satellite imagery of the wakes of islands (e.g., Thomson et al. 1977). There was almost no evidence of quasi-periodic kinks associated with vortices, although some elongated weak velocity region behind the ridge was present during the study period.

#### 2) ENHANCEMENT OF PRECIPITATION

Figure 10 shows the turbulence kinetic energy derived from the Doppler velocity. The data are average during the study period. The turbulent wake area adjacent to the ridge is clarified, and was associated with the precipitation enhancement in the reflectivity on the leeward slope (see Fig. 5 (a)). A physical mechanism has not been determined without more data, however, a possible factor contributing to the precipitation enhancement in the mountain wake flows may be the seeder-feeder effect; that is, the turbulence may produce the concentrations of supercooled cloud droplets and snow particles from the upstream may be enhanced by riming in the region of wake flows.

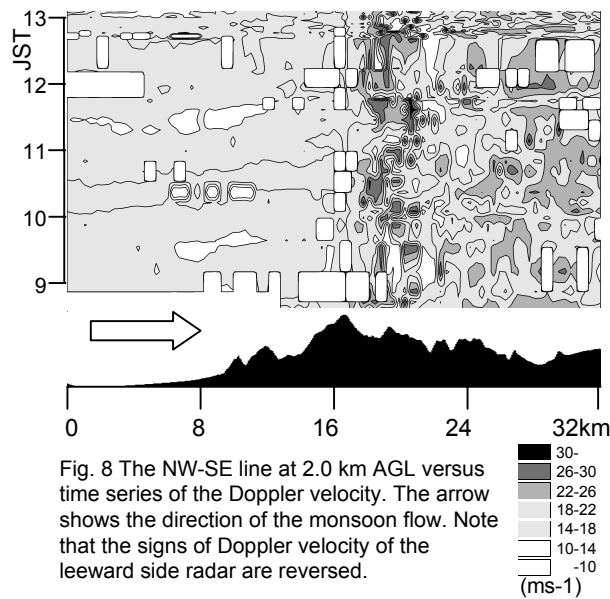


Fig. 8 The NW-SE line at 2.0 km AGL versus time series of the Doppler velocity. The arrow shows the direction of the monsoon flow. Note that the signs of Doppler velocity of the leeward side radar are reversed.

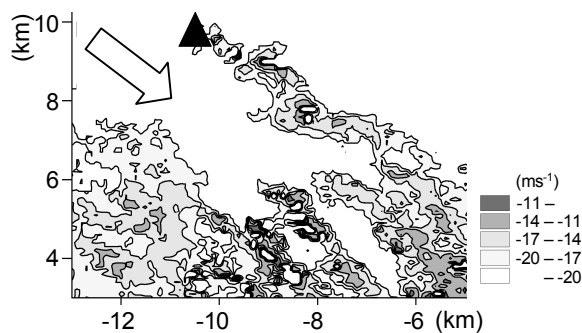


Fig. 9 Example of PPI scan (Doppler velocity) of the leeward radar at 0934 JST. The location of the ridge is superimposed (triangle). The arrow shows the location of the direction of the monsoon.

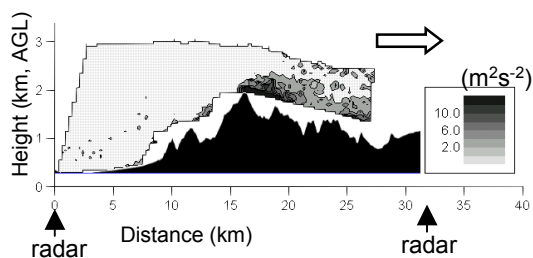


Fig. 10 The turbulence kinetic energy derived from the Doppler velocity along the NW-SE vertical plane.

## 5. Summary

This paper documents the flows and precipitation around the Mikuni Mountains, Japan, for a case of the winter monsoon (relatively steady northwesterly flow). The high-resolution Ka-band Doppler radars were deployed on the windward and leeward slopes, respectively, and composites were constructed from RHI scans oriented toward each other. The results are as follows.

(1) Relatively laminar flows on the windward side became turbulent when the flows past the mountain ridge.

(2) Precipitation enhancement in the radar reflectivity was observed on the windward slope and the turbulent wake area on the leeward slope.

(3) On the lee side, an acceleration and deceleration of the horizontal wind speed were observed, suggesting the flow accelerated to a supercritical speed followed by a hydraulic jump-like transition.

(4) PPI scans of the Doppler velocity suggest the presence of an unsteady separated wake in which vortex shedding occurred.

(5) The behavior of echo cells on the windward side were qualitatively consistent with the upstream Froude number ( $Fr$ ): When  $Fr$  was relatively large, the flow accelerated and the echo height became thicker over the ridge, and echo pattern suggests that the cells flowed almost directly across the mountain ridge. When  $Fr$  was small, the flow decelerated and the echo height became thinner over the ridge, and cells flowed around the summit in the case.

*Acknowledgements.* The project is supported by the Ministry of Land, Infrastructure, and Transport of Japan Government.

## REFERENCES

- Iwanami, K. R. Misumi, M. Maki, T. Wakayama, K. Hata and S. Watanabe, 2001: Development of a multiparameter radar system on mobile platform. Proc. Preprinted, *30th Conf. on Radar Meteorology*, Amer. Meteor. Soc., 104-106.
- Murakami, M., M. Hoshimoto, N. Orikasa, K. Kusunoki, and Y. Yamada, 2000: Microstructure and precipitation processes in a stable orographic snow cloud over the Mikuni Mountains in Central Japan. *Preprints, 13th International conference on cloud and precipitation*, 371-374.
- Thomson, R. E., J. F. R. Gower, and N. W. Bowker, 1977: Vortex streets in the wake of the Aleutian Islands. *Mon. Wea. Rev.*, **105**, 873-884